Iccs16, Porto

Smart EMI monitoring of thin composites structures

Pierre Selva, Olivier Cherrier, Valérie Budinger , Frédéric Lachaud and Joseph Morlier

Ce projet est cofinancé par l'Union européenne. L'Europe s'engage en Midi-Pyrénées avec le Fonds européen de développement régional.

Overview

1. Goals of the SAPES project
2. Short focus on … our Multilevel approach and EMI experimental setup
3. Piezo properties identification by solving inverse problem
4. Damaged zone localisation (Probabilistic Neural Networks)
5. Conclusion and future works

1.Goals

Goals

Structural Health Monitoring (SHM) method for in-situ damage detection and localization in Carbon Fibre Reinforced Plates (CFRP).

Impact detection in composites thin structures: in aeronautic ➔
Problem of Birdstrike, ice etc...

The detection is achieved using the ElectroMechanical Impedance (EMI) technique employing piezoelectric transducers as high-frequency modal sensors.

Numerical simulations based on the Finite Element (FE) method are carried out so as to simulate more than 100 damage scenarios.

Simple damage model is used in order to limit computation time (high discretization, high frequency bandwith) and from exploring all domain with few points (100) we construct an approximation (surrogate model using ANN) of damage localization versus selected (pertinent) indicators from EMI analysis.

Damage metrics are then used to quantify and detect changes between the electromechanical impedance spectrum of a pristine and damaged structure

2.Short Focus on…

Short Focus on… Multilevel approach

The main goal of his paper is to develop a multiscale localisation method that can be applied to a global structure (e.g. aircraft door), a subpart (composite plate) or a structural detail (stiffener).

The amount of data that needs to be generated to ensure a good generalization depends on the structure under study. For instance, if a global structure is considered, a large database of E/M impedance signatures relative to different localized single damage is ultimately required.

Simulations will be utilized so as to construct a significant database relative to the subpart problem in order that PNN well generalized (supervised approach)

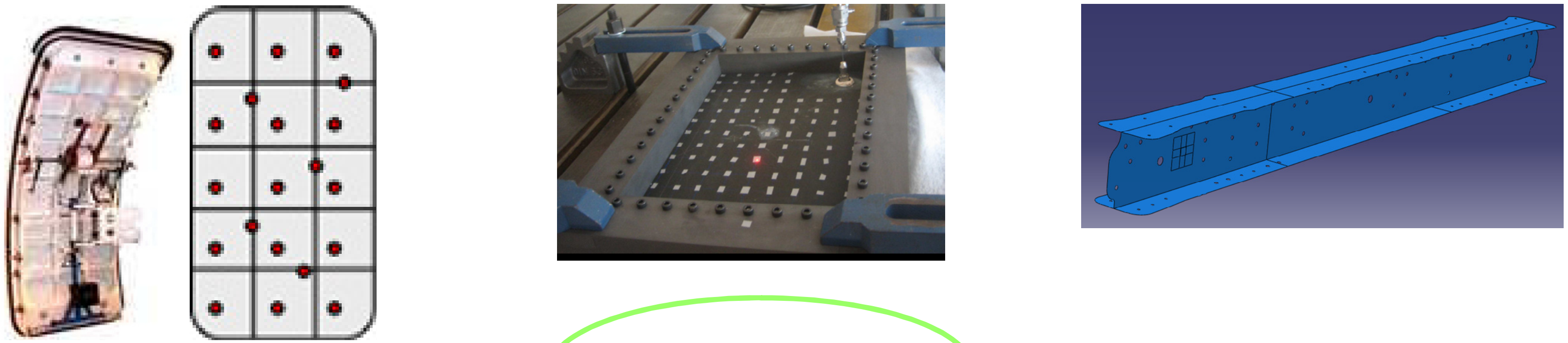

(a) Aircraft door (b) Composite plate (c) Stiffener

Figure 1: Modeling principle of the EMI technique from global to details

ICCS16

Short Focus on… Modeling principle of the EMI

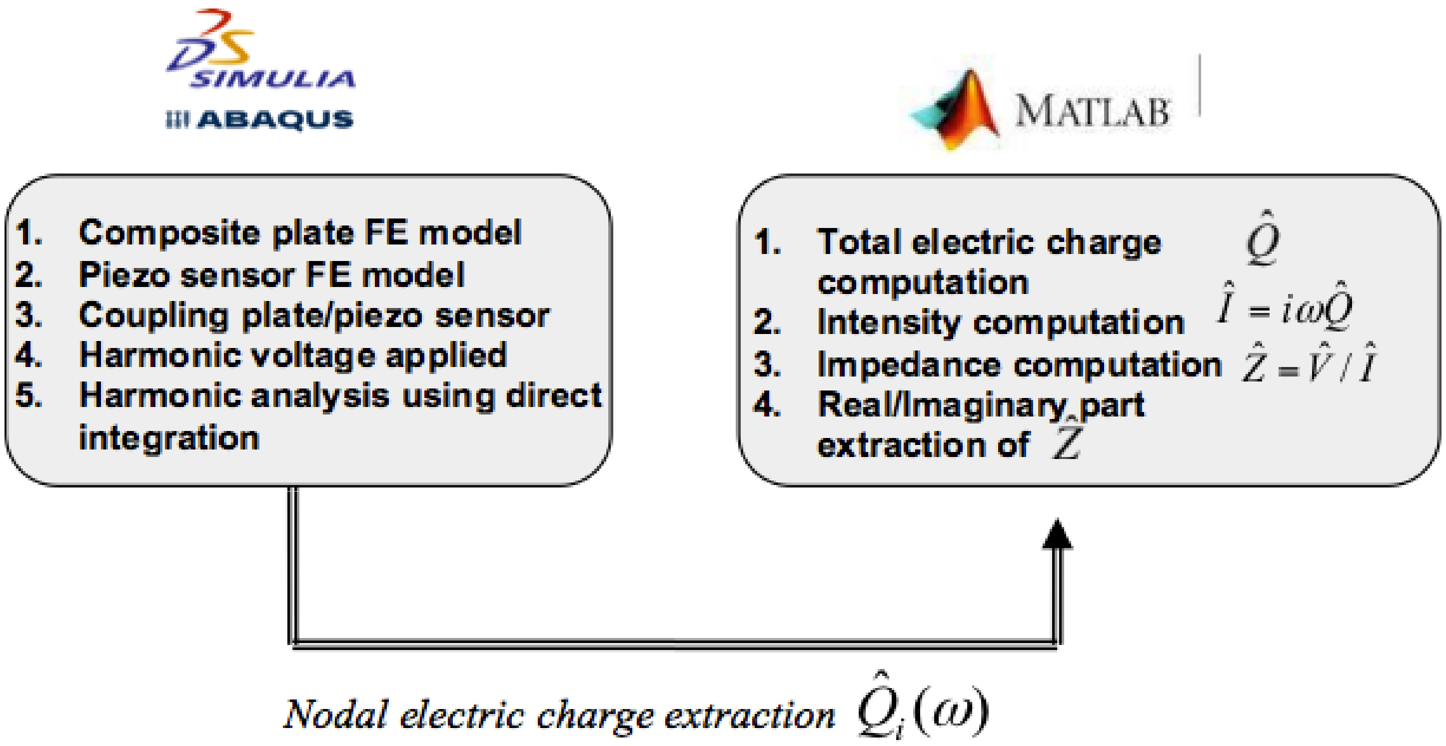

In order to generate a significant dataset relative to different damage localization
, a coupled-field finite-element (FE) model of the EMI technique is developed in Abaqus [8]

The FE model permits to compute electrical reaction charges over each sensor electrode,
which are then imported into Matlab [9] to derive the corresponding E/M impedance signature.

The resulting impedance spectrum is then processed to derive damage indicators.
Finally, these damage metrics are used as inputs to train, validate and test the ANN.

Short focus on … EMI measurement

Experimental setup

• 3 PZT mounted on composite plateT700 M21 (PI : PIC 151) : 10x10x0.5mm
• bi composants Epoxy/Argent (EPO-TEK® E4110) : thickness 0.3 mm

• Measurement system: Impedancemeter PsimetriQ N4L modèle 1700
+ Active Head (integrated shunt)

EMI principle:

→ Broadband excitation
- voltage measurement PZT
- voltage measurement shunt
- PZT intensity :
- Impedance estimation:

$$I_{PZT}(\omega) = \frac{V_{shunt}(\omega)}{R_{shunt}}$$

$$Z_{PZT}(\omega) = \frac{V_{PZT}}{I_{PZT}(\omega)}$$

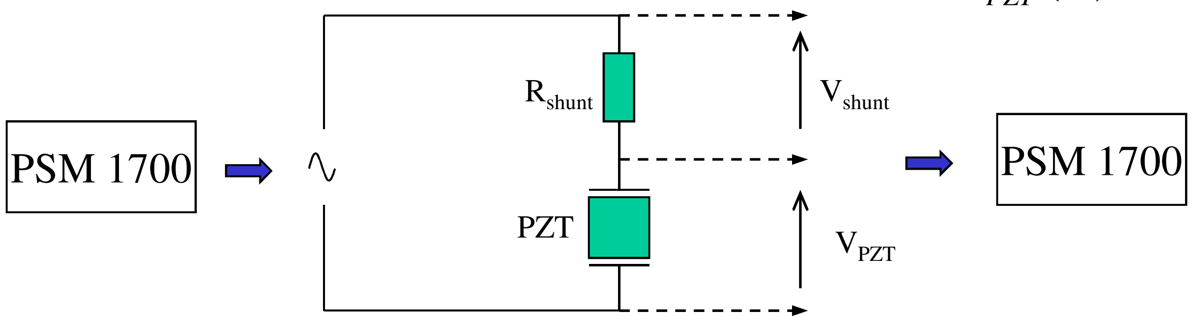

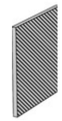

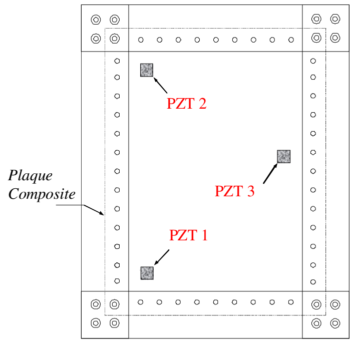

3.Piezo updating

Piezo updating (1)

Piezoceramics properties exhibit statistical fluctuations within a given batch and a variance of the order of 5-20% in properties

Therefore it becomes really important to accurately identify the behavior of the piezoelectric sensors as we solely depend upon these transducers to predict the mechanical impedance of the structure

Identification of piezo material properties solving inverse problem

- → From experimental data
- → Fit Analytical model *(Bhalla & Soh, 2004 & 2008)*

Coef. diélectric

$$\left[\varepsilon^T\right] = \begin{bmatrix} \varepsilon_{11}^T & 0 & 0 \\ 0 & \varepsilon_{11}^T & 0 \\ 0 & 0 & \boxed{\varepsilon_{33}^T} \end{bmatrix}$$

Coef. Dielectric loss

$$\bar{\varepsilon}_{33}^T = \varepsilon_{33}^T (1 - \boxed{\delta} i)$$

Constants piezo.

$$[d] = \begin{bmatrix} 0 & 0 & 0 & 0 & d_{15} & 0 \\ 0 & 0 & 0 & d_{15} & 0 & 0 \\ \boxed{d_{31} \quad d_{31}} & & d_{33} & 0 & 0 & 0 \end{bmatrix}$$

Structural Damping

$$\boxed{\eta}$$

Coef. correction

$$\boxed{C}$$

Low freq ID(<10kHz) — Coef. diélectric, Coef. Dielectric loss

Around resonant frequency ID (≈200kHz) — Constants piezo., Structural Damping, Coef. correction

Piezo updating (2)

Impedance of a free PZT is :

Bhalla & Soh (2004, 2008)

$$\bar{Y} = \frac{\bar{I}}{\bar{V}} = 4\omega j \frac{l^2}{h}\left[\boxed{\bar{\varepsilon}_{33}^T} + \frac{2\boxed{d_{31}^2}\,Y^E(1+\boxed{\eta}\,i)}{(1-\nu)}\left(\frac{\tan \boxed{C}\kappa l}{C\kappa l} - 1\right)\right]$$

Low Frequencies

$\tan(C\kappa l)/C\kappa l \rightarrow 1$

$$\bar{Y}_{libre} = G_{f,qs} + B_{f,qs}\,j = \left(\frac{8\pi l^2 f \boxed{\varepsilon_{33}^T}\boxed{\delta}}{h}\right) + \left(\frac{8\pi l^2 f \boxed{\varepsilon_{33}^T}}{h}\right) j$$

Exp measurements

2 linear functions of f

$$B_{f,qs}^* = \frac{B_{f,qs}h}{8\pi l^2} = \varepsilon_{33}^T f \qquad G_{f,qs}^* = \frac{G_{f,qs}h}{8\pi l^2 \varepsilon_{33}^T} = \delta f$$

→ Identification of: ε_{33}^T *et* δ

Piezo updating (2: results)

Example : PZT n°1

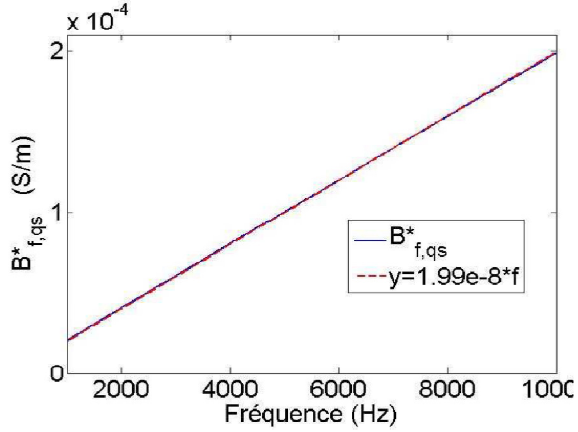

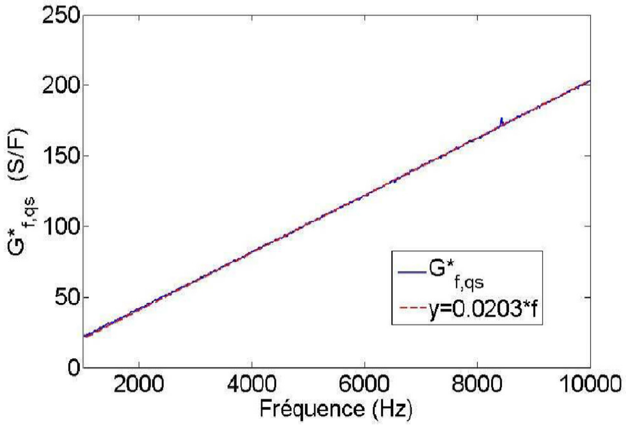

Résults for 3 PZT :

	PZT 1	PZT 2	PZT 3
$\varepsilon_{33}^{T}\ (10^{-8}\,F/m)$	1.991	2.034	2.009
Δfournisseur	6.7%	9.0%	7.7%
δ	0.0203	0.0207	0.0204

Impedance Re(Z) of PZT n°1

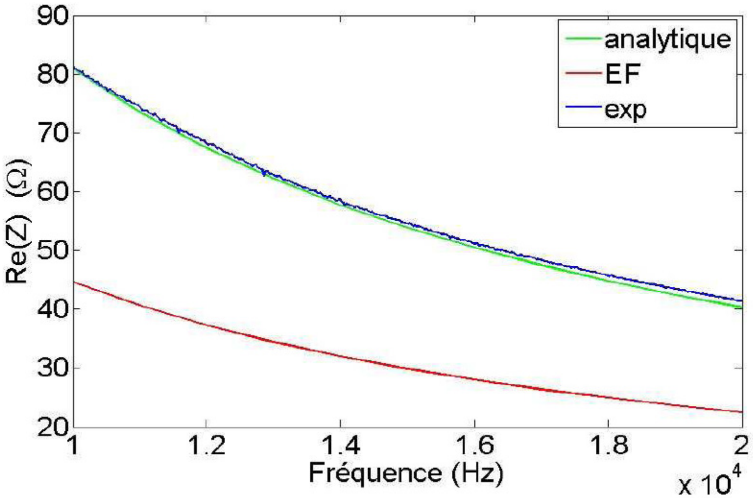

→ bias due to non implemented dielectric losses in abaqus

Piezo updating (3)

Parameters to be identified: $d_{31},\ \eta\ et\ C$

$$\bar{Y} = \frac{\bar{I}}{\bar{V}} = 4\omega j \frac{l^2}{h}\left[\bar{\varepsilon}_{33}^T + \frac{2\boxed{d}_{31}^2 Y^E(1\boxed{+\eta}\,i)}{(1-\nu)}\left(\frac{\tan \boxed{C}\kappa l}{C\kappa l} - 1\right)\right]$$

Nonlinear quadratic function to be minimized

$$\min \sum \left(\underbrace{\bar{Y}(f,\boxed{d_{31},\eta,C})}_{\text{Analytic model}} - \underbrace{\bar{Y}_{\exp}(f)}_{\text{Exp measurements}}\right)^2$$

Analytic model

Exp measurements

Piezo updating (3: results)

PZT n°1

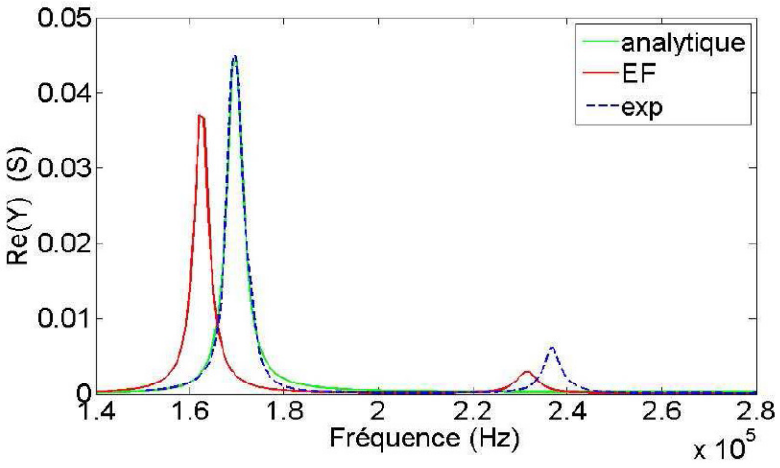

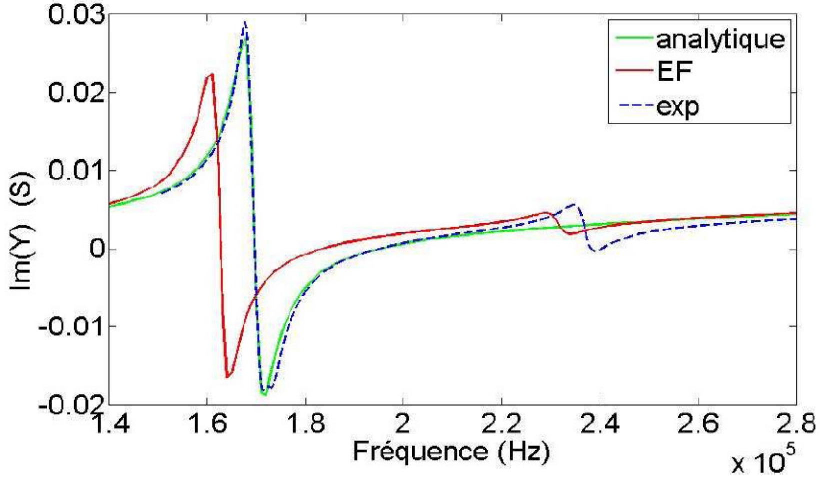

→ Excellent numerical experimental correlation

	d_{31} (10^{-10})	$\Delta fournisseur$	η	C	C_1	C_2	*corrélation analytique/exp.*
PZT 1	-1.8373	14.1%	0.0224	0.8681	-	-	0.998
PZT 2	-1.7718	17.2%	0.0185	-	0.8588	0.8909	0.976
PZT 3	-1.7716	17.2%	0.0219	-	0.8594	0.8787	0.992

→ It exists important difference between PZT manufacturer's material data and identified data

4.0. The idea behind supervised ANN: generalization

Damaged zone identification

Generalization is the process of recognize unknown cases from database of indicators (inputs) versus damage localisation (outputs)

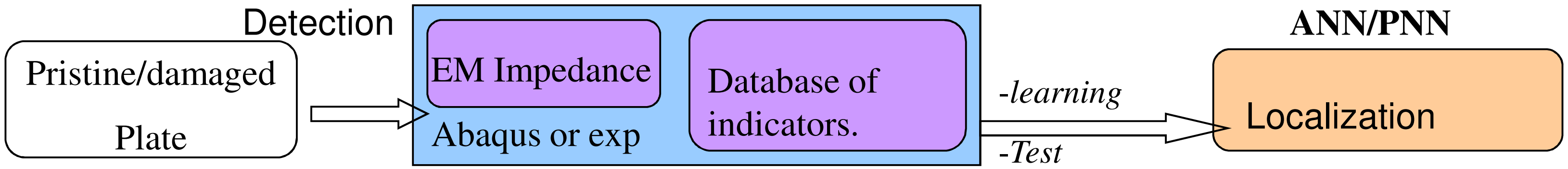

• Supevised ANN (previous studies) : discrete prediction (x,y) ➔ induce sometimes large errors

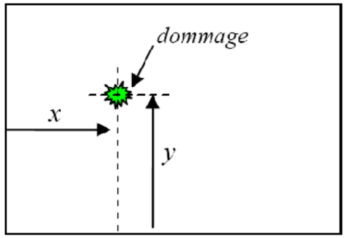

• ICCS studies: Damaged zone prediction (classification problem well adapted to industrial constraints and multilevel approach)

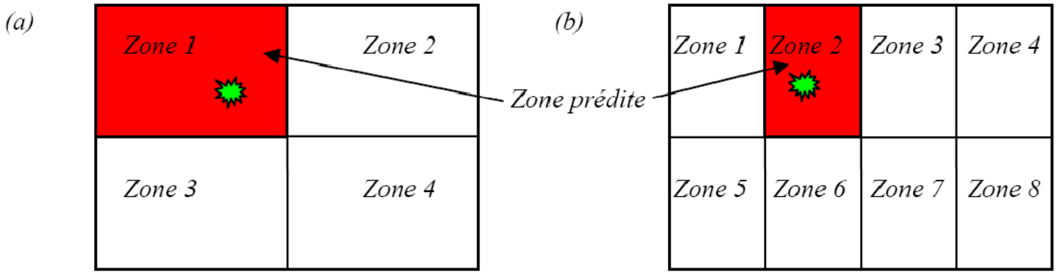

Classification Problem → PNN

PNN A simple example: 1 database of 4 examples (learning vectors)

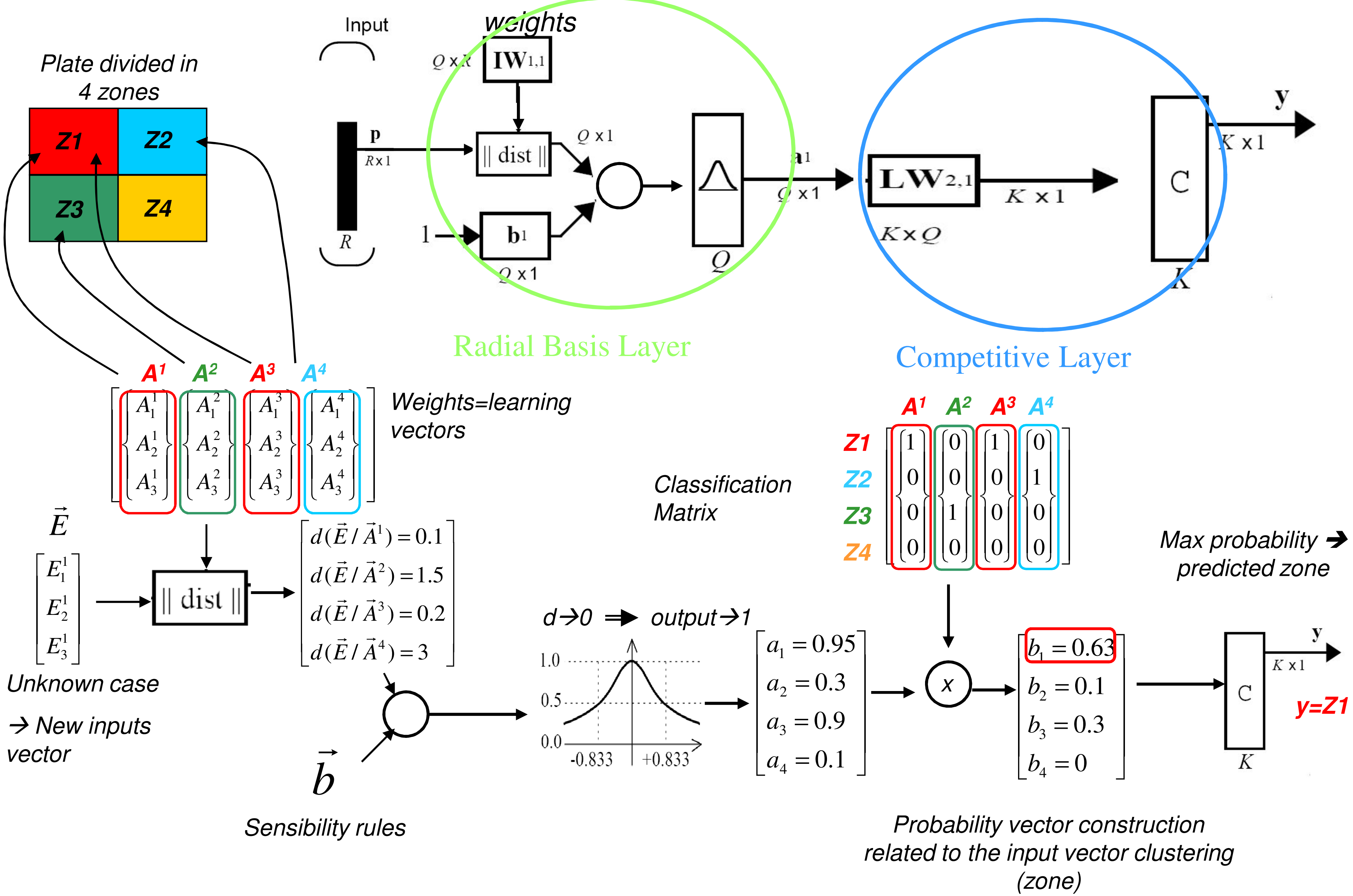

4.1. Parametric approach (The big Picture)

4.1. Parametric approach (The big Picture)

Example : PZT n°1

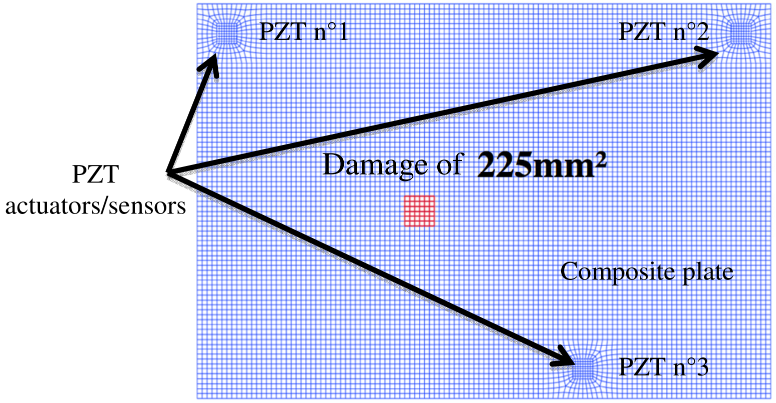

A finite-element model consisting of three piezoceramic patches (designation PIC151) of dimensions 10x10x0.5mm^3 bonded onto a composite plate (200x290mm^2) .

The composite layup is composed of 12 plies of carbon/epoxy prepreg T700/M21 for a total thickness of 3mm.

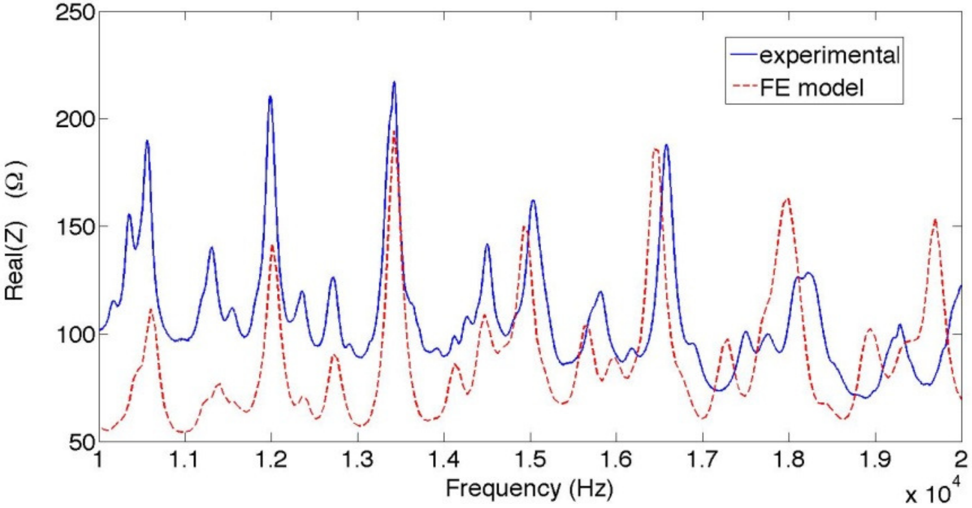

Comparison of real part frequency response of impedance (experimental vs numerical model) for a pristine composite plate measured from PZT n°1.

Parametric approach (2)

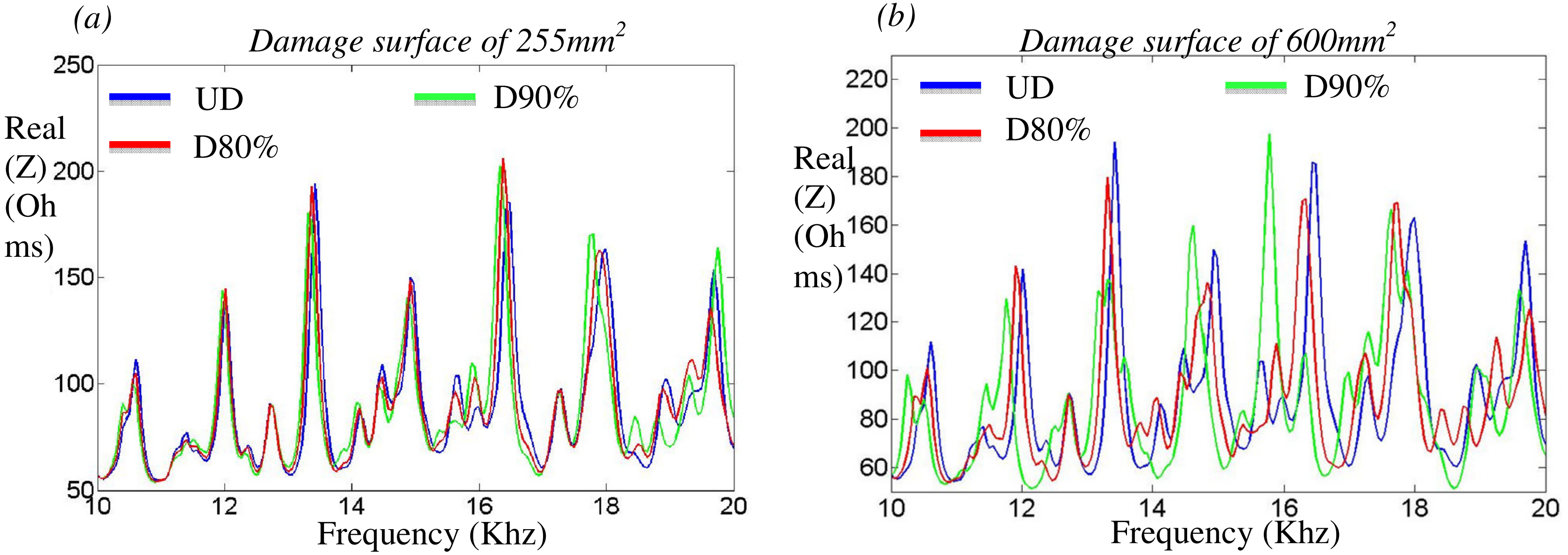

Figure 6. Comparison of impedance spectra predicted by the FE model at the PZT n°1 terminals between undamaged (UD) and damaged (D80% or D90%) composite plates. (a) and (b) Plots corresponding to a damage surface of 225mm^2 and 600mm^2 respectively.

PNN Strategy : Mapping

- 3 damage zone surfaces: 100, 225, 600mm² ➔ 3 independant database
- 2 severities: decrease of 80% ou 90% de $E_2/E_3/G_{12}/G_{13}/G_{23}$
- Border zones deleted from database
- Generation of database (learn 80%)
- Test of 100 networks (Results: mean of 5 best)
- Cross (random) validation 20%

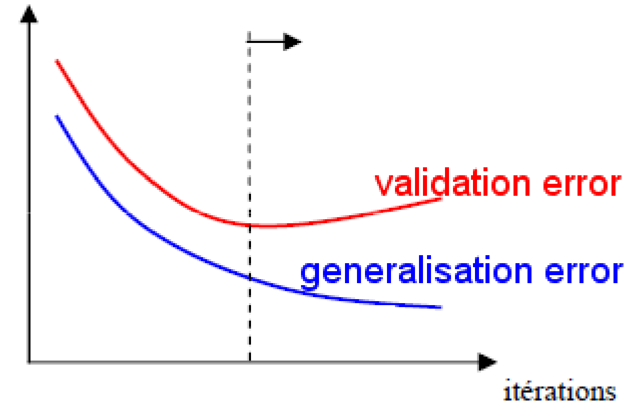

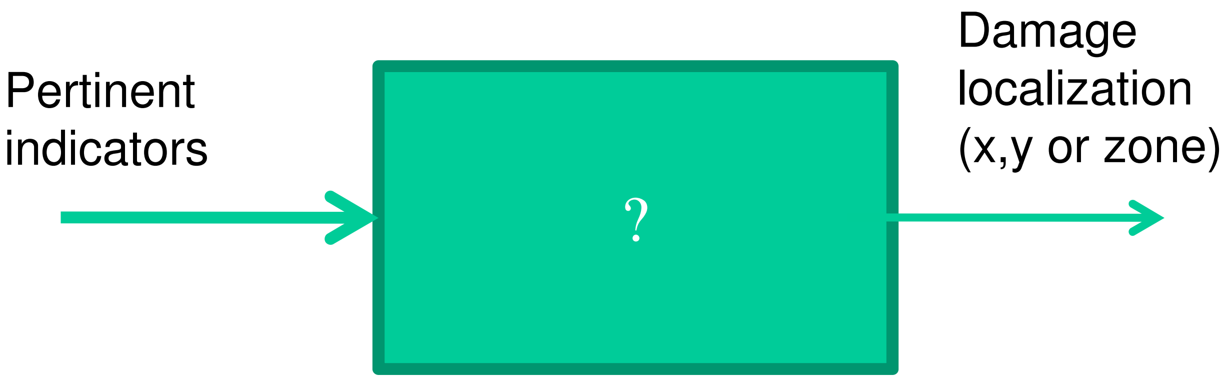

PNN Preliminary tests

Inputs choice is predominant in the classification results

→ Inputs are defined from comparison of impredance spectrums (2 successive states :damaged/pristine)

- Corrélation Coef. (Re(Z)) → 1
- Area substraction (Re(Z) & Im(Z)) → 2
- Quadratic mean (Re(Z) & Im(Z)) → 2
- Root mean square deviation (Re(Z) & Im(Z)) → 2

$$RMSD = \sqrt{\frac{\sum_N \left[\mathrm{Re}(Zi) - \mathrm{Re}(Z_i^0)\right]^2}{\sum_N \left[\mathrm{Re}(Z_i^0)\right]^2}}$$

7 indicators from Bibliography for each PZT
➔ 21 indicators

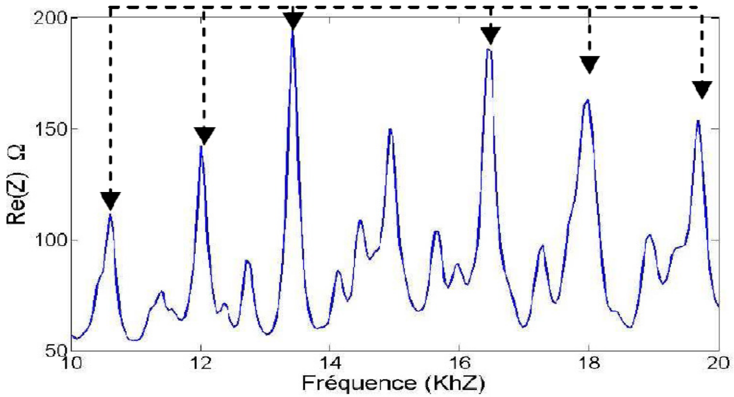

Using only these indicators 47% of the networks are able to well classifiying 90% of the new damages

When we add 22 new indicators (frequency shifts)

85% of the networks are able to well classifiy 90% of the new damages

PNN Preliminary tests

Example of pertinent indicator RMSD

- As it can be expected, the higher the surface of damage, the higher the RMSD index is. The same conclusion can be drawn as regard the damage severity.

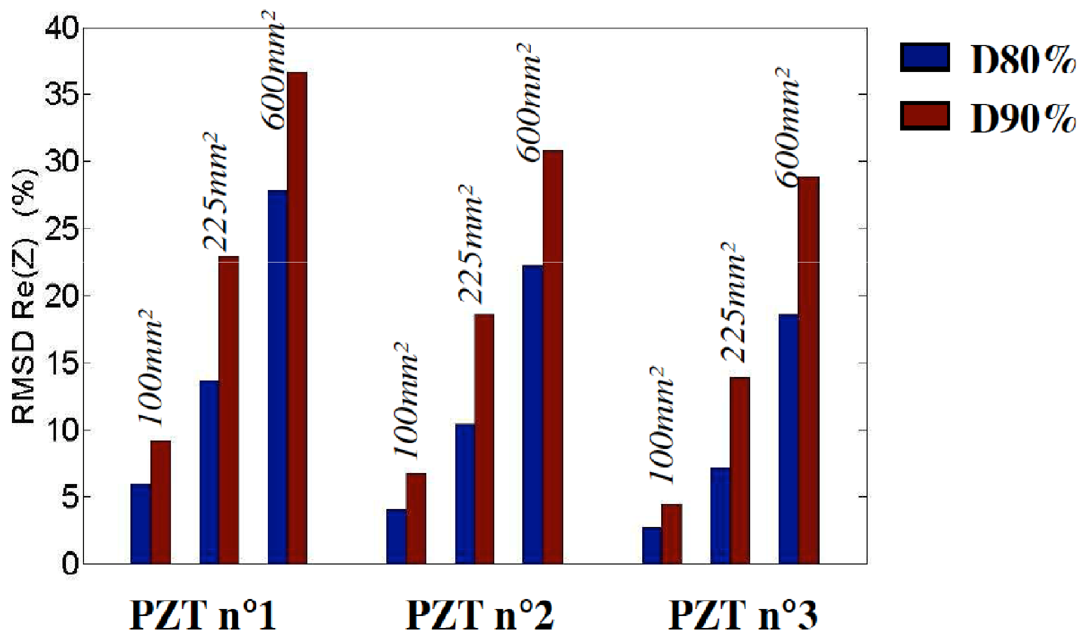

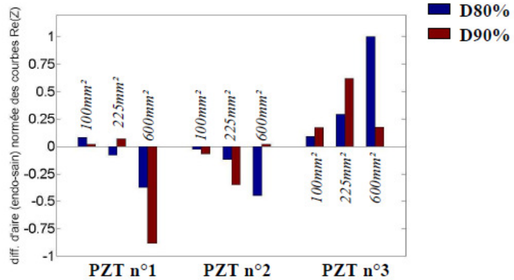

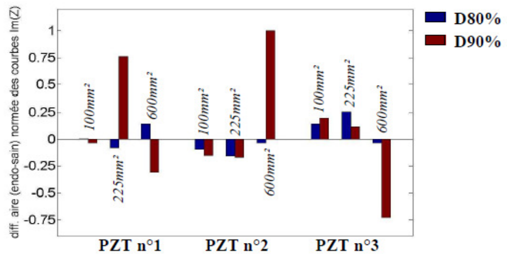

➔**The other selected indicators more complex behavior that will help PNN to distinguish between damages having similar RMSD value but different localization.**

4.2. Database creation from numerical analysis (Damage scenarii on Abaqus)

PNN

High damage area: 600mm²

Learning base 118 damages, no frequency shifts as input vectors

- Test base 20 unlearned (new) cases

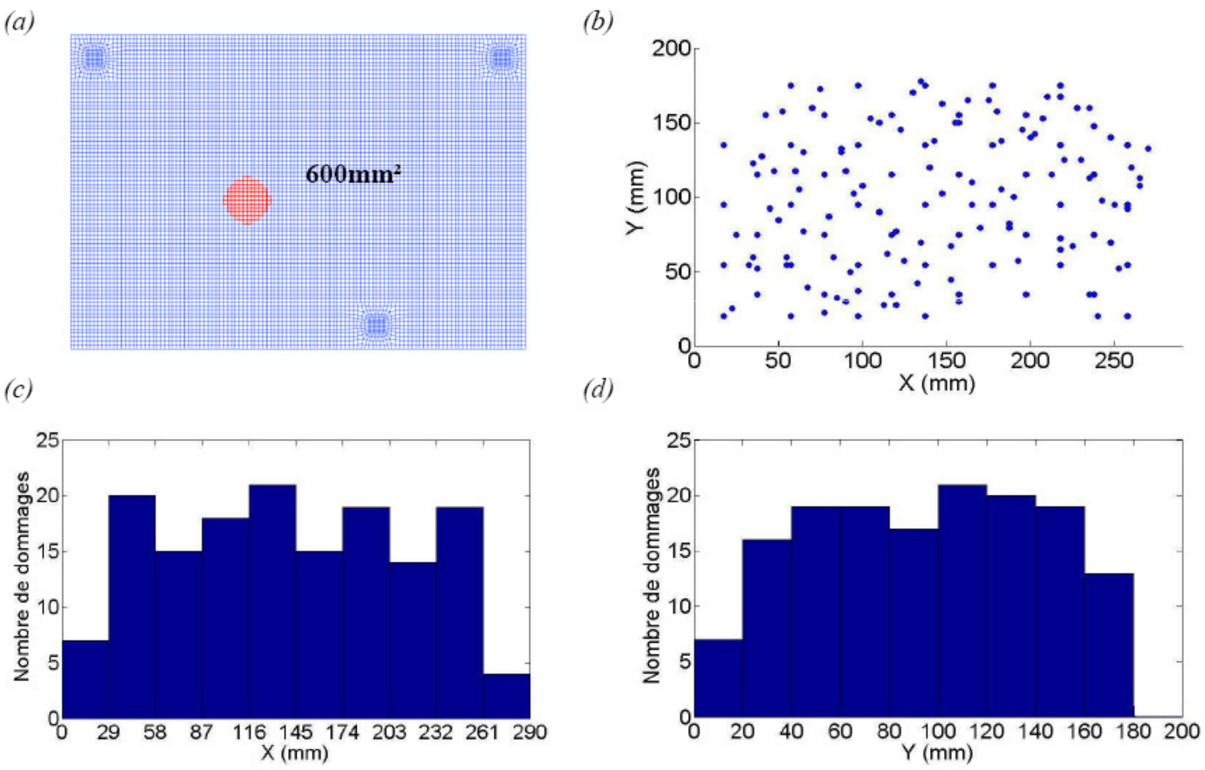

Random discrete location of damages

Histogram (X and Y)

PNN

High damage area: 600mm²

Dommages 600mm², sévérité d'endommagement 80%

	Nombre de dommages correctement localisés							
	10/10	9/10	8/10	7/10	6/10	5/10	4/10	<4/10
localisation	*Nombre de réseaux sur 100*							
1/4 de plaque	30	39	21	10	0	0	0	0

69% of the networks can predict 90% of the unknonw (new) damage location

90% f the networks can predict 80% of the unknown (new) damage location

10 new damages example

1/4 plate clustering

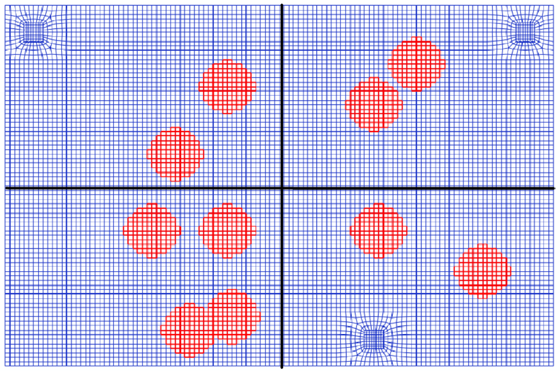

→ Very High variation of 21 indicators: can we reduce the input vector size ???

PNN

High damage area: 600mm²

Dommages 600mm², sévérité d'endommagement 80%

Entrées considérées	Dim.	*Nombre de dommages correctement localisés* 10/10	9/10	8/10	7/10	6/10	5/10	4/10	<4/10
		Nombre de réseaux sur 100							
Toutes	21	30	39	21	10	0	0	0	0
RMSD Re(Z)	3	18	27	29	18	5	3	0	0
RMSD + Aire Re(Z)	6	27	39	26	4	3	1	0	0

→ PCA : reduced input vector containing RMSD Area diffrence of Re(Z) – dimension 6 – has the same performance than the all vector : For High damage area some indicators are correlated

PNN

Medium damage area: 225mm²

- Learning base 245 damages
- Test base 20 unknown (new) cases

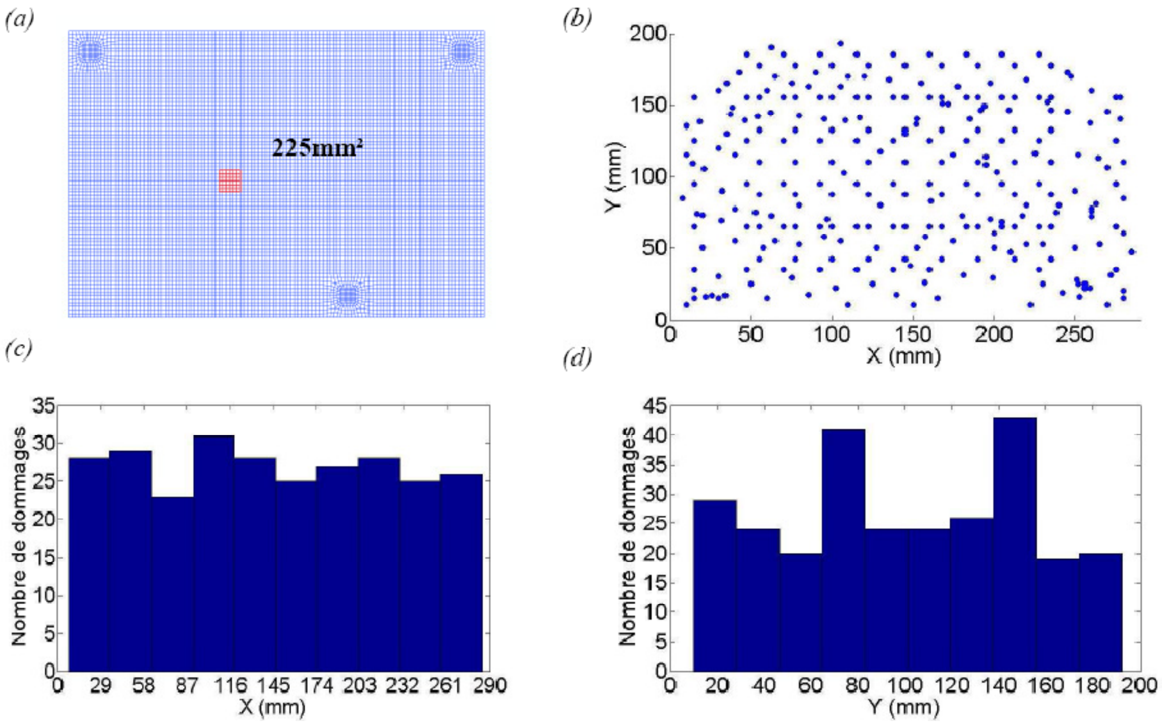

Random discrete location of damages

Histogram (X and Y)

PNN

Medium damage area: 225mm²

Dommages 225mm², sévérité d'endommagement 80%

	Nombre de dommages correctement localisés							
	20/20	19/20	18/20	17/20	16/20	15/20	14/20	<14/20
localisation	*Nombre de réseaux sur 100*							
1/4 de plaque	24	36	25	10	3	2	0	0
1/8 de plaque	10	27	24	21	12	4	2	0

85% of the networks are able to predict 80% of the 20 new unknown damages

61% of the networks are able to predict 90% of the 20 new unknown damages

Some examples

1/4 plate

20 examples

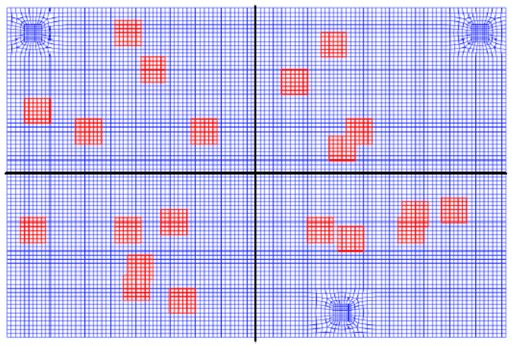

1/8 plate

20/20

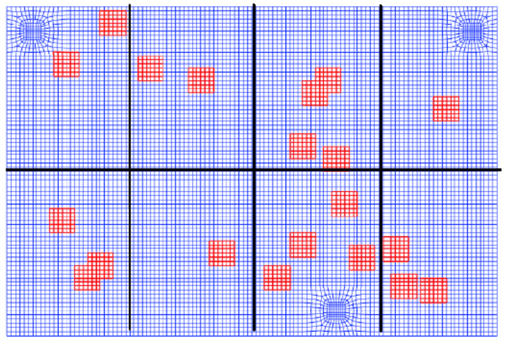

→ Due to computational time limits we did only hundred of scenarri, not sufficient to generalized even adding frequency shifts indicators

PNN

Low damage area

Damages 100mm²

- Learning base165 damages , Test base 20 unknown (new) cases

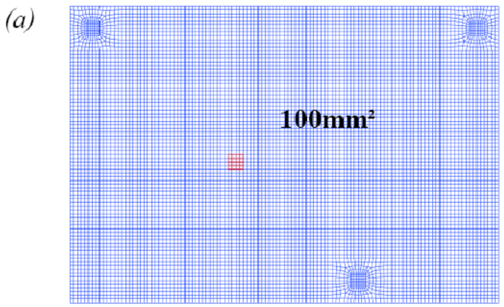

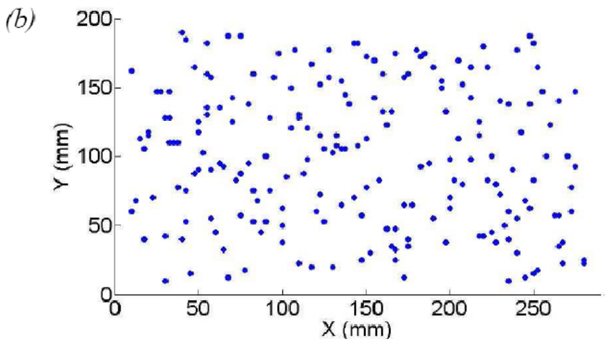

Random discrete location of damages

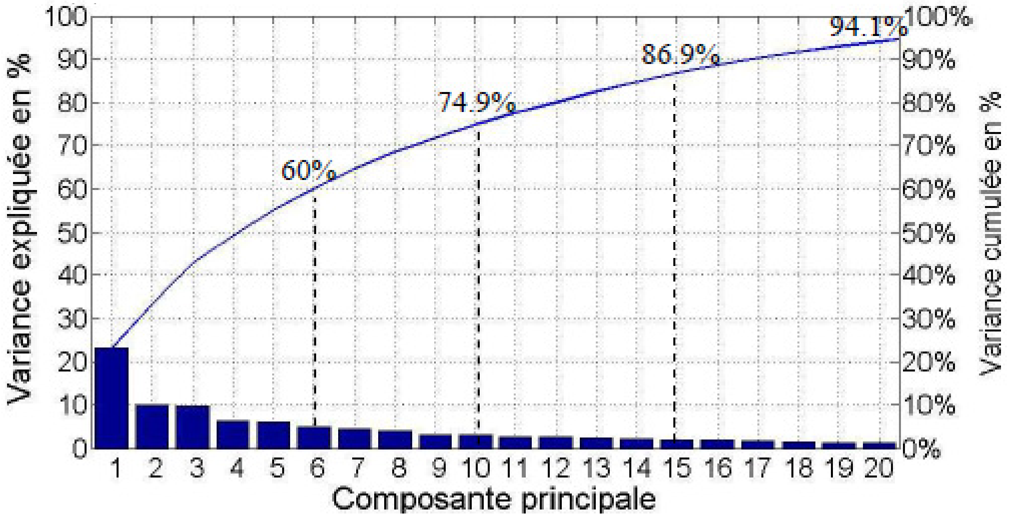

PCA answers that all indicators are needed …

→ **lower performance of the networks only of 35% of the networks are able to localize**

→**Indicators shifts are too small, database too small, local effects ?**

4.3. Experimental results (unknown cases)

4.3. Experimental EMI

- <u>Plate n°3:</u>

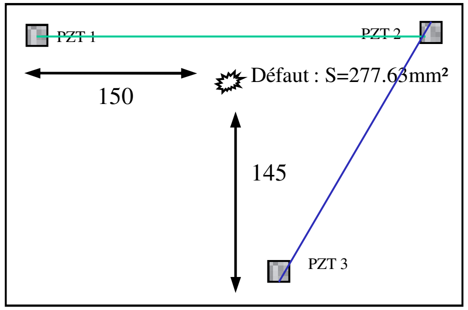

Damage Localization

Max	Déplacement (mm)	Effort (N)	Temps d'impact (ms)
	-5,63	6067,33	5,28

Données d'impact E=20J

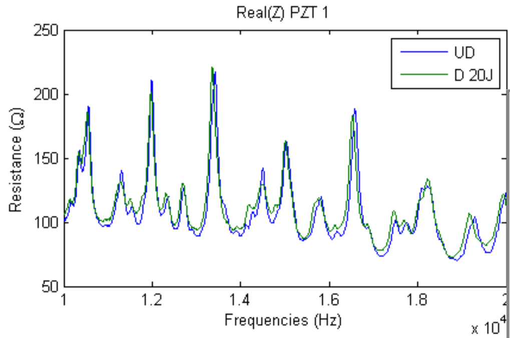

3 EMI curves

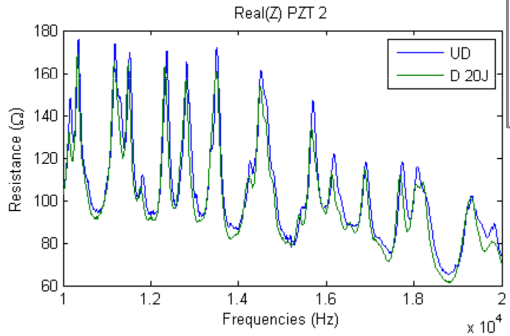

RMSD

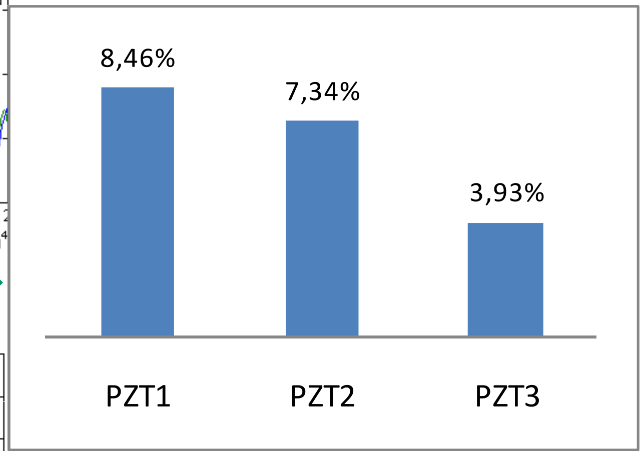

Shift in frequency

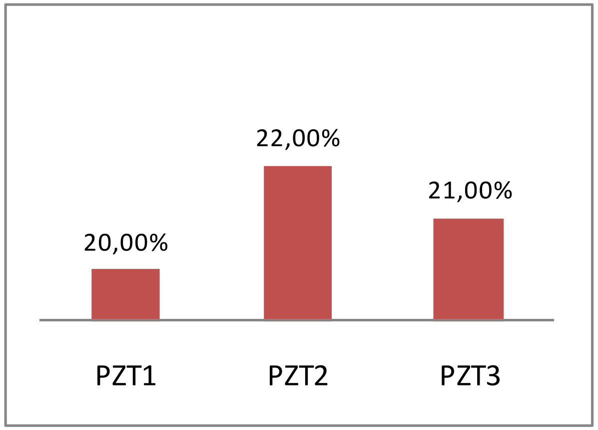

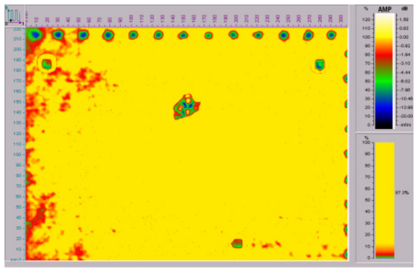

Amplitude

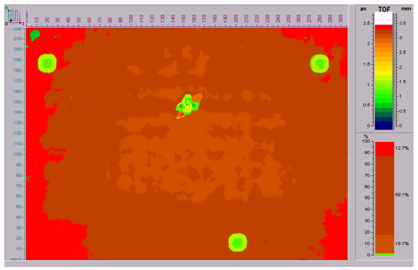

Profondeur

US and : Cscan resolution 0.3mm

4.4. Final Results of classification

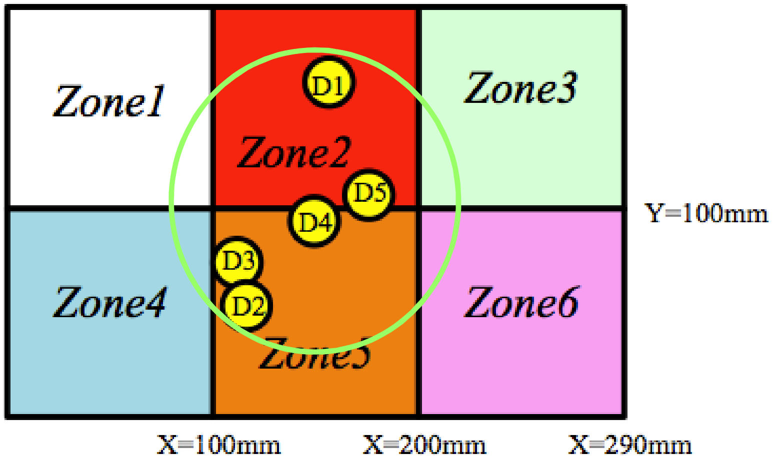

Experimental constraints: central zone for impact drop test machine

So we only have 5 experimtal points (unknown cases) to be recognized by the PNN

Plate n°	*Damage center (x,y)*	*US Surface*	*Real zone*	*Predicted zone*
1	(150,145)	≈280mm²	**2**	**2**
2	(116,52)	≈381mm²	5	4
3	(110,87)	≈399mm²	**5**	**5**
4	(145,95)	≈380mm²	**5**	**5**
5	(177 ,105)	≈ 366mm²	2	4

D2 and D5 Problem of Border zones deleted from database…

5. Concluding remarks

EMI is able to detect and localize damage in composites plates, Our coupled FEM approach is interesting for exp/num EMI correlation

Piezo updating is an important phase in the monitoring process

3 surface of damages : 100, 225, 600mm² ➔ 3 different database, and 3 performances of PNN

Supervised ANN→ x,y location prediction with reliability close to half damage size

PNN → Damaged zones localization(1/4 ou 1/8 of plate)

Ability to predict correct zone for all kind of damages

Good generalization for medium and large damage area

Futur works ➔ Increase of damage scenarii for better generalization (small damage area)

Clustering of optimal zone (a priori information)

From ISO SURFACE NETWORKS to ISO ENERGY of IMPACT …

we need to know the predicted damage area versus location for each type of impact.